ELSEVIER

Contents lists available at ScienceDirect

# **Brain Stimulation**

journal homepage: www.journals.elsevier.com/brain-stimulation





# Epidural magnetic stimulation of the motor cortex using an implantable coil

Kyeong Jae Lee<sup>a</sup>, Jae-Won Jang<sup>a</sup>, June Sic Kim<sup>b</sup>, Sohee Kim<sup>a,\*</sup>

- a Department of Robotics and Mechatronics Engineering, Daegu Gyeongbuk Institute of Science and Technology (DGIST), Daegu, Republic of Korea
- <sup>b</sup> Clinical Research Institute, Konkuk University Medical Center, Seoul, Republic of Korea

#### ARTICLE INFO

Keywords:
Magnetic stimulation
Epidural stimulation
Low-intensity magnetic stimulation
Neuromodulation
Motor evoked potential
Implantable coil

#### ABSTRACT

Background: Magnetic stimulation, represented by transcranial magnetic stimulation (TMS), is used to treat neurological diseases. Various strategies have been explored to improve the spatial resolution of magnetic stimulation. While reducing the coil size is the most impactful approach for increasing the spatial resolution, it decreases the stimulation intensity and increases heat generation.

*Objective:* We aim to demonstrate the feasibility of magnetic stimulation using an epidurally implanted millimeter-sized coil and that it does not damage the cortical tissue via heating even when a repetitive stimulation protocol is used.

Methods: A coil with dimensions of  $3.5 \times 3.5 \times 2.6$  mm<sup>3</sup> was epidurally implanted on the left motor cortex of rat, corresponding to the right hindlimb. Before and after epidural magnetic stimulation using a quadripulse stimulation (QPS) protocol, changes in the amplitude of motor evoked potentials (MEPs) elicited by a TMS coil were compared.

Results: The experimental group showed an average increase of 88 % in MEP amplitude in the right hindlimb after QPS, whereas the MEP amplitude in the left hindlimb increased by 18 % on average. The control group showed no significant change in MEP amplitude after QPS in either hindlimb. The temperature changes at the coil surface remained <2 °C during repetitive stimulation, meeting the thermal safety limit for implantable medical devices.

Conclusion: These results demonstrate the feasibility of epidural magnetic stimulation using an implantable coil to induce neuromodulation effects. This novel method is expected to be a promising alternative for focal magnetic stimulation with an improved spatial resolution and lowered stimulus current than previous magnetic stimulation methods.

### 1. Introduction

Magnetic stimulation, represented by transcranial magnetic stimulation (TMS), is a therapeutic technique that stimulates the brain with electric fields induced by intense magnetic fields without exposing metallic or conducting electrodes to the body. Coils used for magnetic stimulation are generally large enough to cover one hemisphere of the human head to generate a magnetic field strong enough to induce neural responses [1]. Due to its considerable size, such a coil is limited in precisely stimulating cortical regions with a high spatial resolution. In order to overcome this issue, various coil shapes such as figure-eight, or assistive techniques such as navigation systems have been introduced [2, 3]. Nonetheless, the area affected by the coil is larger than the target region to be stimulated, making stimulation of a pericentral region around the target region unavoidable. The coil size has to be reduced to

increase the spatial resolution of magnetic stimulation. However, this downsizing involves two trade-offs: increased heat generation and decreased stimulation intensity [4]. The resistance increases as the coil becomes smaller, generating more heat during repetitive stimulation. The number of stimuli per unit time must be reduced to avoid excessive heat generation, which may cause ineffective stimulation. While shortening the pulse width is another approach to reducing heat generation [5], it is limited in practical applications by the minimum duration required to stimulate neurons and the characteristics of the TMS system generating pulses with a capacitive discharging method [6]. In addition, downsizing the coil limits the current intensity, which hinders inducing a suprathreshold stimulus to elicit neural responses.

In our preliminary experiments, we aimed to directly elicit motor evoked potentials (MEPs) using the implanted coil, but two major limitations prevented this. One was a misalignment between the direction

E-mail address: soheekim@dgist.ac.kr (S. Kim).

<sup>\*</sup> Corresponding author.

of the electric field generated by the coil and the orientation of the axons of targeted pyramidal neurons. This misalignment results in a higher stimulus threshold for obtaining a direct response during magnetic stimulation [7-10]. Achieving a minimal threshold to evoke MEPs requires proper alignment, which was unattainable because the axons of pyramidal neurons are oriented perpendicular to the cortical surface, while the electric field generated by the epidural coil runs parallel to the axons. Consequently, a higher intensity of electric field was necessary to evoke MEPs. However, generating such a strong electric field posed another practical constraint related to heat generation. The intensity of the electric field is proportional to the current flowing through the coil, and higher currents led to excessive heat production in the coil. If a field strong enough to evoke MEPs were generated, the resultant heat would risk causing thermal damage to surrounding brain tissue. As a result, we shifted our focus towards exploring stimulation protocols that could modulate neural plasticity without the risk of heat-induced tissue

Given these boundaries, recent studies have explored alternative approaches such as low-intensity stimulation using TMS in the perifocal area. These studies demonstrate that subthreshold stimulation modulates cortical excitability and alters gene expression and neural pathways, for which the modulation of internal calcium signaling is a key mechanism [11-19]. Based on these studies, low-intensity repetitive TMS (LI-rTMS) using coils with a reduced size has recently emerged as an alternative magnetic stimulation method [12,13]. LI-rTMS using a coil with dimensions of  $8 \times 8 \text{ mm}^2$  (diameter  $\times$  height) was shown to modulate the amplitude of MEPs [14], synaptic plasticity in the motor cortex [15], and neuronal activity via in vivo intracellular recording of pyramidal neurons in the somatosensory cortex [16], and c-Fos expression using a temporal interference stimulation system [17]. LI-rTMS was also shown to modulate the frequency of seizure-like events using a coil with a tapered core [18] and the amplitudes of MEPs and somatosensory evoked potentials using a C-shaped coil [19]. The common feature of these studies is that the coils were placed outside the head with a particular distance between the coil and the head. As the distance between the coil and the targeted cortical region increases, the strength of the electric field decreases, and the distribution of the field broadens, resulting in decreased focality.

Another approach for magnetic stimulation uses an intracortical coil to maximize the stimulation intensity by minimizing the distance between the coil and neurons. These types of coils are typically fabricated by microfabrication processes [8,20,21] or have shanks on which thin Pt-Ir wires are formed in a bent shape [8,22,23]. These coils are inserted into the cortical layers containing pyramidal cells. Magnetic stimulation using such coils with several hundreds of micrometers has the advantage of stimulating a focal area. However, it has an inevitable limitation that inserting the coil into the cortex causes irreversible cortical damage.

To elicit or to modulate neural responses, it is necessary to create a change in electric field in the targeted cortical region. Previous studies have reported that an electric field intensity exceeding 10 V/m achieved neuromodulation in motor evoked potential [14,19]. To attain such high-intensity electric field using a miniaturized coil, options include reducing the distance between the coil and the target region or using a high-intensity current pulse. Bonmassar et al. and Bernardo et al. show the feasibility of magnetic stimulation with current intensities in the mA scale [7,24]. These results were achievable since the coil approached the targeted region as close as possible. In contrast, epidural implantation restricted narrowing the distance between the coil and the targeted region, leaving increasing the current intensity as the sole viable option.

Given these considerations, using a small coil placed on the surface of the cortex would represent a trade-off between improving the focality of magnetic stimulation and avoiding the inevitable damage caused by penetrating the cortical tissue. However, placing a coil in contact with the brain surface may be limited by the potential tissue damage caused by hyperthermia generated by the coil [25]. Histological findings demonstrated that temperatures of  $\geq$ 44 °C caused thermal damage in

the normal brain tissue of non-human primates [26]. The maximum temperature increase for implantable medical devices stipulated by the International Organization for Standardization (ISO) is 2  $^{\circ}$ C [27]. Therefore, the heat generated at the coil surface should be less than this limit to be acceptable for magnetic stimulation using an implanted coil.

In this study, we introduce a novel method to maximize the intensity of the induced electric field by implanting a small coil on the cortical surface without penetrating the brain tissue. The coil was implanted to cover the motor cortex of rat to demonstrate the feasibility of epidural magnetic stimulation. Our results show that the amplitude of MEPs before and after the stimulation protocol was successfully modulated. The temperature increase at the coil surface during repetitive stimulation was also confirmed to remain within the thermal safety limit.

### 2. Methods

# 2.1. Coil and pulse generator for MEP modulation

We used a small coil with dimensions of  $3.5\times3.5\times2.6~\text{mm}^3$  (Fig. 1), which was previously used to demonstrate the feasibility of magnetic stimulation for peripheral nerves [28]. This coil had an inductance of 1 mH and a resistance of 16  $\Omega$ . It comprised 256 turns, the bare wire diameter was 50  $\mu$ m (44 AWG), and the diameter including insulation was 70  $\mu$ m. In order to prevent the potential current leakage, the coil was insulated with a thin (50  $\mu$ m thick) layer of electrically resistive epoxy (832HT, MG Chemicals, ON, Canada). The coil was connected to a two-pin connector (51021-02, Molex, Lisle, IL, USA) through two wires connected to a pulse generator.

The pulse generator consisted of a function generator (AFG3022B; Tektronix, Beaverton, OR, USA) and a power amplifier (HSA4014; NF Corp., Yokohama, Japan), which allowed it to generate an arbitrary pulse shape with a high current amplitude up to 7.2 A. The pulse shapes used in this study replicated the monophasic pulses used in commercial TMS, which have a rising time of 70  $\mu$ s [29–31]. However, unlike TMS pulses, the generated pulses lacked a long tail after the peak (Fig. 2(a)). This shortened pulse reduced the excessive energy consumption in the coil, resulting in less heat generation [31–33]. The amplitude and shape of the current pulses were measured using an oscilloscope (MSO-X 3054T; Keysight, Santa Rosa, CA, USA) and a current probe (1147B; Keysight, Santa Rosa, CA, USA) to confirm the consistency of coil characteristics before and after applying the stimulation protocol.

### 2.2. Heat measurement

The temperature at the coil surface was measured to ensure thermal safety using a thermistor (SS6L; BIOPAC Systems Inc., Goleta, CA, USA) before coil implantation. Since the coil was implanted inside the head, the thermistor could not measure the temperature changes during *in vivo* experiments. Instead, we measured the coil surface temperature in air by placing the thermistor in contact with the coil. Since biological tissues have higher thermal conductivities than air, the temperature rise at the surface of an implanted coil is expected to certainly be lower than the measurement in air, as evidenced by previous experimental results [32, 34]. Then, the stimulus shown in Fig. 2(a) was applied to the coil for 10 min, with current intensities increased from 2.4 A to 7.2 A with a step of 1.2 A. The maximum stimulus intensity was decided by the current amplitude that would increase the temperature by < 2 °C based on the ISO guideline for implantable medical devices [27].

# 2.3. Simulation of electromagnetic field

Simulations were conducted using COMSOL Multiphysics 5.5 (COMSOL, Stockholm, Sweden) to estimate the magnitude of the induced electric and magnetic fields. A 3D rat head model, reconstructed from computed tomography (CT) scanning images, was imported into the software to mimic the *in vivo* environment. Tissue properties such as

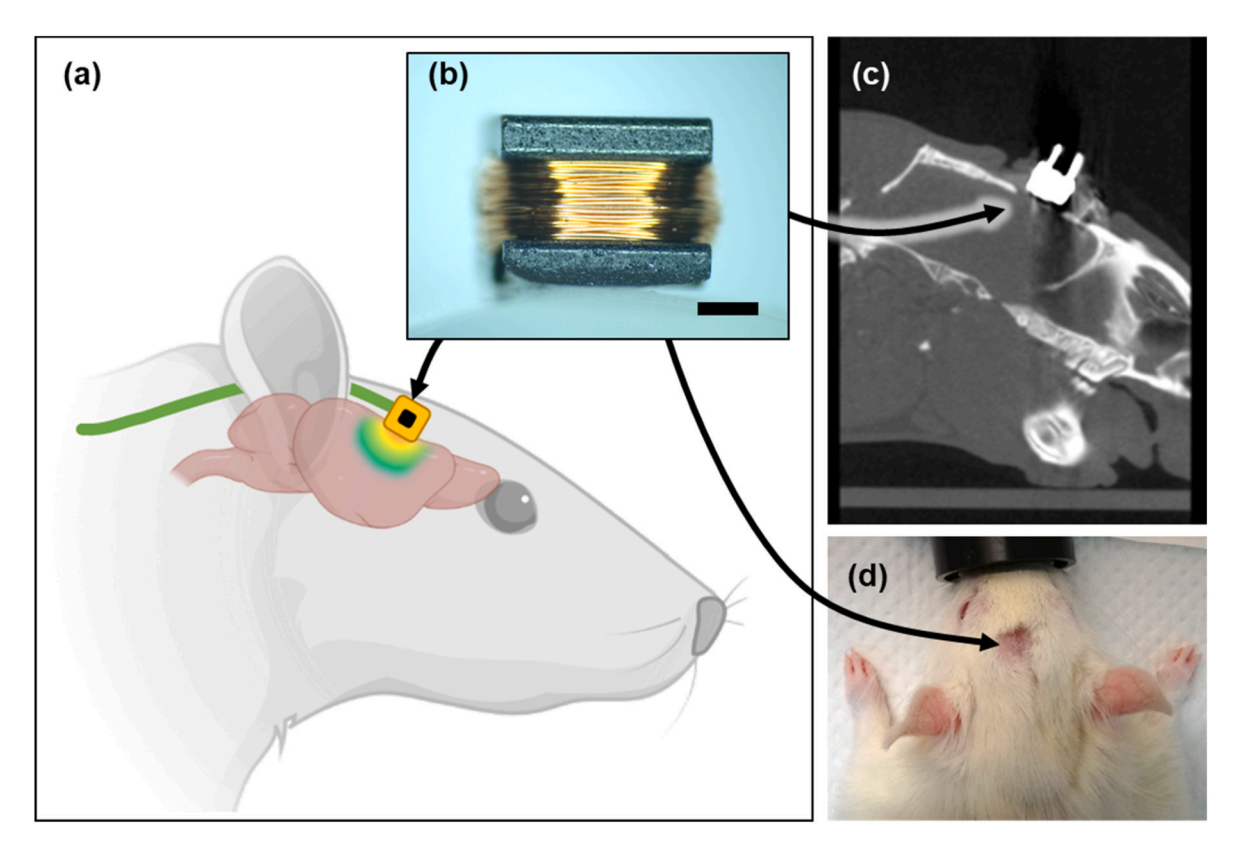
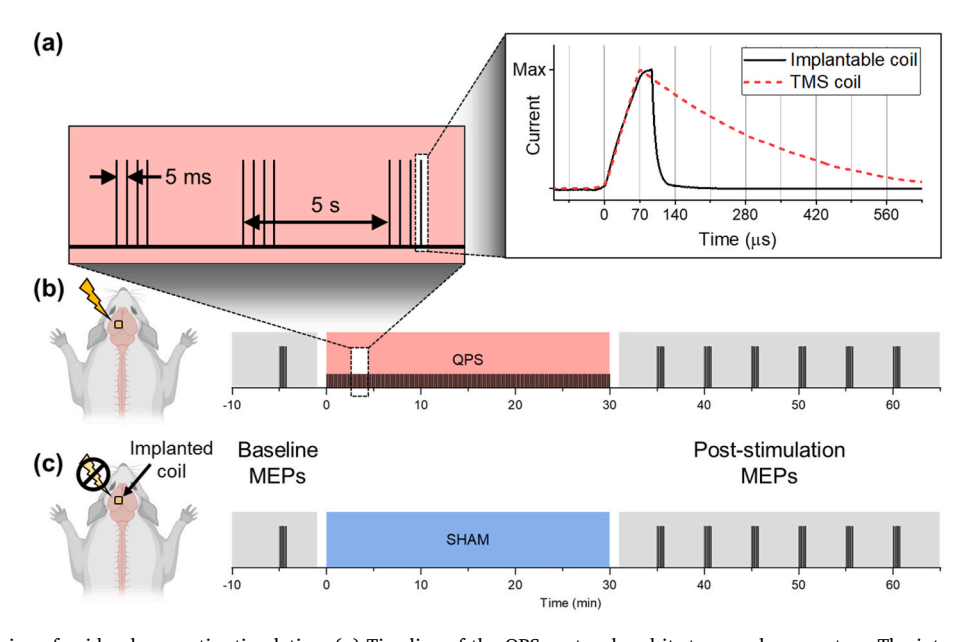


Fig. 1. Coil implantation to a rat for epidural magnetic stimulation. (a) Schematic illustration of coil implantation: A coil (wire: yellow, magnetic core: black) is implanted epidurally on the targeted cortical region, with connecting wires (green) placed subcutaneously. (b) Prototype coil used in experiments; the scale bar is 1 mm. (c) CT image of the implanted coil in sagittal plane. (d) Recovered rat after coil implantation. The arrows indicate where the coil is implanted. (For interpretation of the references to color in this figure legend, the reader is referred to the Web version of this article.)



**Fig. 2.** Experimental design of epidural magnetic stimulation. (a) Timeline of the QPS protocol and its temporal parameters. The inter-stimuli and inter-train intervals were 5 ms and 5 s, respectively. The enlargement on the right compares monophasic current pulses used for the implantable coil (black solid line) and a TMS coil (red dashed line). The protocols used for (b) QPS and (c) no stimulation conditions are illustrated. Before applying stimulation, MEPs were measured as the baseline. After the conditioning, ten MEPs were recorded consecutively with an interval of 5 min to observe the post-stimulation effect. (For interpretation of the references to color in this figure legend, the reader is referred to the Web version of this article.)

electrical conductivity, relative permittivity, and relative permeability for the brain, cerebrospinal fluid, and skull were adopted from a previous study [35]. The electric field induced by the coil was calculated in

the frequency domain at a frequency of 3.571 kHz, which corresponds to a period of a quadruple pulse with a rise time of  $70 \mu s$ . The amplitude of the current applied to the coil was determined to be the highest value

that satisfied the criterion of thermal safety limit, resulting in the maximum applicable current of 6 A (see Section 3.1).

### 2.4. Coil implantation

Male Sprague–Dawley rats (300–500 g) were divided into the experimental (n=5) and control (n=4) groups. Rats were housed with a 12/12 h light/dark cycle and given food and water *ad libitum*. All animal experiments were approved by the Institutional Animal Care and Use Committee of the Laboratory Animal Resource Center at Daegu Gyeongbuk Institute of Science and Technology (approval number: DGIST-IACUC-23041405).

Under anesthesia with 2 % isoflurane, the head was fixed using a stereotaxic frame (KOPF 902; KOPF Instruments, Tujunga, CA, USA). Following the scalp incision, a piece of skull in a size of  $4\times 4$  mm and centered at +2.0 mm lateral and +2.0 mm posterior to the bregma was removed by craniectomy. The exposed cortical region corresponded to the motor cortex of the right hindlimb [36–39]. The coil was placed epidurally, and its winding direction was aligned anterior-to-posterior. Then, the coil was fixed by covering it with dental resin (Ortho-Jet; Lang Dental, Wheeling, IL, USA). Two wires connected to the coil were placed subcutaneously under the dorsal skin, leaving only a two-pin connector outside the body through a small dorsal hole at the center of the trunk for the connection to the pulse generator. The incised scalp was sutured, and then the rats were allowed to recover for a week with appropriate treatments using antibiotics and painkillers. The schematic illustration of coil implantation and its CT image are shown in Fig. 1.

### 2.5. Anesthesia during epidural magnetic stimulation

The rat implanted with the coil was briefly anesthetized for 10 min under 2 % isoflurane for catheterization of the tail vein for intravenous propofol infusion. Propofol was chosen as the anesthetic drug since it has been reported that stable MEPs were obtained for up to 4 h when using it [40–43]. After catheterization, bolus injection of propofol at an infusion rate of 1 mg/kg/min was given over 10 min. Isoflurane was discontinued for 5 min after the start of propofol loading. After bolus injection, the infusion rate was changed to 700  $\mu$ g/kg/min to maintain the anesthesia for sedation throughout the experiment for up to 2 h. Oxygen at 1 L/min was also supplied via a nose tube throughout the experiment. The conversion of anesthesia was confirmed by observing the twitching of the leg or electromyography signals caused by pinching the toes with tweezers.

### 2.6. Subthreshold repetitive magnetic stimulation with QPS

We used the QPS protocol, a stimulation protocol that delivers four pulses in a burst at a constant interval for epidural magnetic neuromodulation. The details of the QPS used in in vivo experiments are shown in Fig. 2(a). It was reported that the QPS protocol modulated the amplitude of MEPs effectively by changing the inter-stimuli intervals in TMS studies [44,45]. For example, inter-stimulus intervals of 10 ms or less induce long-term potentiation, while intervals of 30 ms-100 ms tend to induce long-term depression in MEPs [44]. The QPS protocol also induced long-lasting synaptic modulation with a subthreshold intensity in in vitro experiments [46]. Based on these results, we set the stimulation parameters as an inter-stimuli interval of 5 ms, an inter-train interval of 5 s, and a total duration of 30 min, resulting in 1440 total pulses (Fig. 2(a)). The current amplitude was set to 6 A to meet the thermal safety criterion (see Section 3.1). MEPs were recorded before and after QPS to observe post-stimulation effects. The baseline was defined as the average amplitude of MEPs recorded 5 min before QPS. After QPS, MEPs were recorded with a 5-min interval. For each session of MEP recording, a stimulus with an intensity of 110 % of the motor threshold (MT) was applied 10 times with an interval of 5 s to elicit MEPs (Fig. 2(b)). For comparison, we also recorded MEPs from the control group that were

not given OPS (Fig. 2(c)).

### 2.7. MEP recording

To record the MEPs, four surface electrodes (Neuroline 70010-K; Ambu, Ballerup, Denmark) were attached to the skin of both hindlimbs after hair removal, and a unipolar needle ground electrode (EL452; BIOPAC Systems Inc., Goleta, CA, USA) was inserted into the tail. MEPs were recorded at a sampling rate of 10 kHz using a recording instrument (MP36; BIOPAC Systems Inc., Goleta, CA, USA). MEPs were elicited using a TMS machine (MagPro R20; MagVenture, Farum, Denmark) with a biphasic sine pulse and a figure-eight coil (MC-B70; MagVenture, Farum, Denmark). During this experiment, the head was fixed using a stereotaxic instrument (SGM-3; Narishige, Tokyo, Japan) to maintain the alignment and distance between the TMS coil and the head. Visual inspection using a camera (Lifecam Studio; Microsoft, Redmond, WA, USA) mounted on top of the experimental cage was also used to confirm the alignment of the TMS coil with the head and to ensure that the position of the head was unchanged after the experiment. The MT was determined when the amplitude of MEPs exceeded 15  $\mu V$ and muscle twitching was observed simultaneously, based on previous studies [42,43,47].

# 2.8. Data analysis

Through visual inspection, the cases where the head was out of alignment at the end of the experiment were excluded from data analysis. Statistical analysis was performed using the MATLAB Statistics and Machine Learning Toolbox (MATLAB 2021a; MathWorks, Natick, MA, USA). In order to compare the experimental and control groups, normalized MEPs were calculated by dividing individual MEP amplitudes by the mean of baseline MEP amplitudes. Two-way analysis of variance (ANOVA) was used to compare the left and right hindlimbs under QPS and sham conditions.

### 3. Results

# 3.1. Heat measurement and maximum applicable current

The temperature changes on the coil surface when QPS was applied for 10 min are shown in Fig. 3. The current amplitude was changed from 2.4 A to 7.2 A with a step of 1.2 A. The highest temperature changes measured for each current amplitude were 0.50 °C, 0.97 °C, 1.41 °C, 1.99 °C, and 3.05 °C, while the average temperature changes were 0.33 °C, 0.55 °C, 1.09 °C, 1.55 °C, and 2.36 °C, respectively. Based on these results, the amplitude of the current ensuring the thermal safety criterion was determined to be  $\leq 6$  A. The measurements also showed that this implantable coil can provide a continuous QPS for a long period. The recovery time required for the temperature to return to the pre-stimulus temperature was determined to be approximately 3 min.

### 3.2. Simulation of electromagnetic field

The simulation results of induced electric and magnetic fields are shown in Fig. 4. Since the coil was sufficiently small, the electric field was induced only in a focal region corresponding to the motor cortex for the left hindlimb. On the brain surface, the highest magnitude of the induced electric field was 25.6 V/m below the coil center. The magnitude of the induced electric field at 1 mm below the coil surface was 10.1 V/m, which is a comparable intensity to those reported eligible to modulate neuronal excitability [14,19]. The magnitudes of magnetic fields were 528 mT and 156 mT below the coil surface and at 1 mm below the coil surface, respectively. Fig. 4(a) shows that the cortical surface region where the magnitude of the electric field was  $\geq$ 20 V/m was 1.5  $\times$  1.5 mm. When the minimally required electric field intensity was lowered to 10 V/m, the region was increased to 3.9  $\times$  2.6 mm and

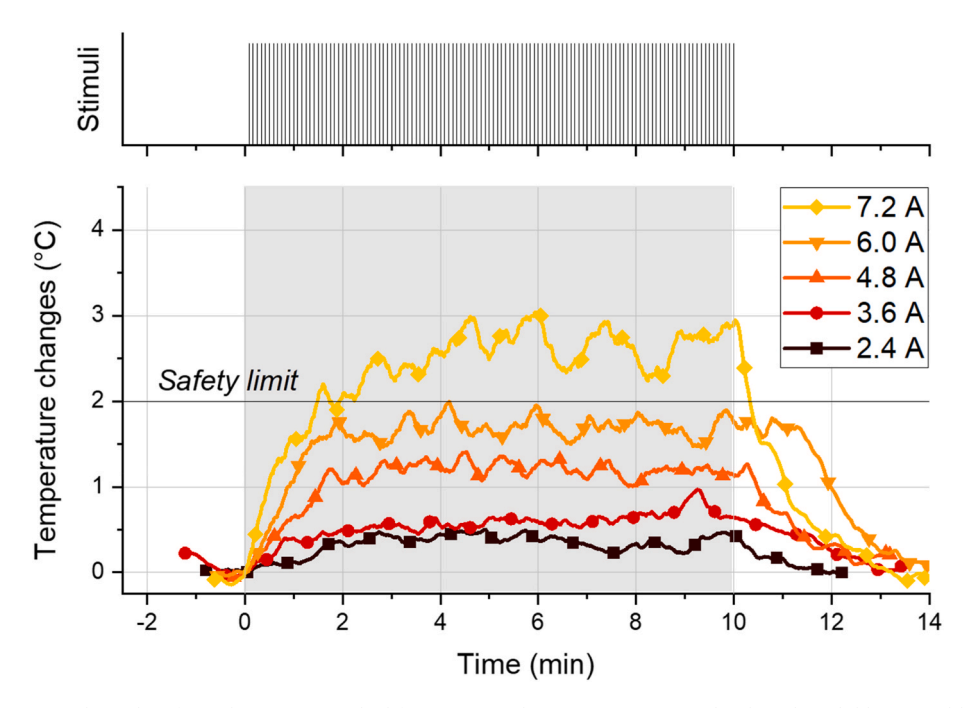


Fig. 3. Temperature changes on the coil surface when QPS is applied for 10 min with varying current amplitudes. The solid horizontal line at 2  $^{\circ}$ C represents the thermal safety limit for implantable medical devices stated in the ISO standard. The temperature change did not exceed the safety limit with a current of  $\leq 6$  A.

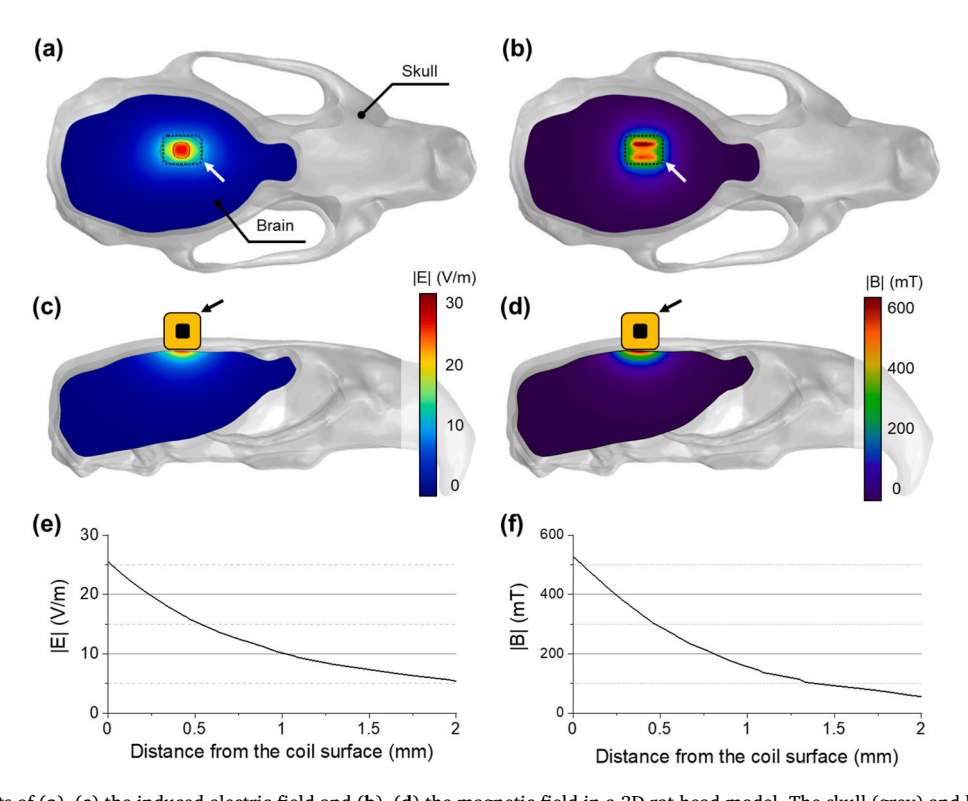


Fig. 4. Simulation results of (a), (c) the induced electric field and (b), (d) the magnetic field in a 3D rat head model. The skull (grey) and brain (blue) are shown in (a), (b) top view and (c), (d) side view. The arrows in (a) to (d) and dashed lines in (a) and (b) indicate the implanted coil. (e) The magnitudes of the induced electric field and (f) magnetic field in the brain are shown as a function of the distance from the coil surface. (For interpretation of the references to color in this figure legend, the reader is referred to the Web version of this article.)

the volume was calculated to be 2.5 mm $^3$ . Since the area of the motor cortex for a hindlimb is approximately 3  $\times$  2 mm [38], the implanted coil is expected to induce changes in neuronal activity at a local area with a sufficient electric field.

## 3.3. MEP measurement

Fig. 5 shows examples of changes in MEP amplitude observed from the right hindlimb with (Fig. 5(a)) and without (Fig. 5(b)) QPS. The amplitude of MEPs was approximately twofold higher after QPS than before QPS. In contrast, the amplitude of MEPs did not change over time

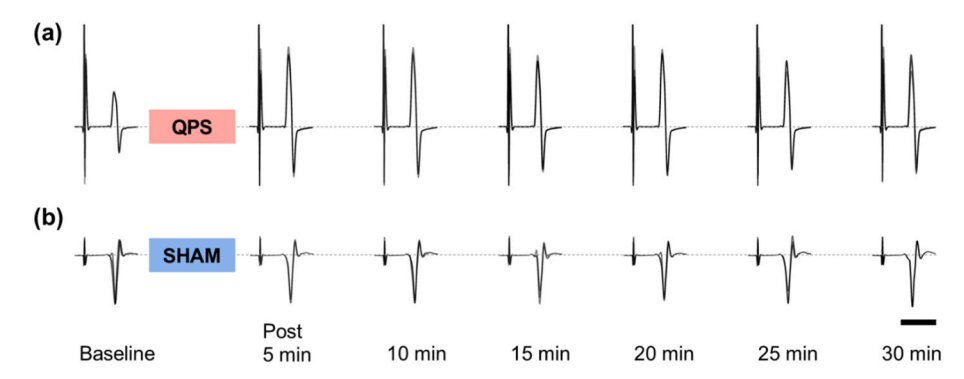


Fig. 5. Examples of temporal changes in MEPs with and without QPS. (a) QPS. (b) No stimulation. The amplitudes of baseline MEPs were normalized in the QPS and sham groups to be commensurable. MEPs after conditioning were then normalized with the baseline MEP under each condition. The scale bar is 10 ms.

when no QPS was applied (sham group). The latencies of MEPs before and after stimulation for both QPS and sham groups were measured as  $8.16\pm0.37$  ms and  $8.21\pm0.75$  ms (mean  $\pm$  standard deviation), respectively. These latencies were consistent with previous studies measuring MEPs in rat hindlimbs using surface or needle electrodes [43, 48].

# 3.4. Time course of MEP changes

Fig. 6 shows the time courses of normalized MEPs for both QPS and sham groups. Fig. 6(a) shows that the MEPs increased in the right hindlimb, which corresponded to the contralateral motor cortex where the implanted coil applied magnetic stimulation. The MEP amplitude was increased by 88 % on average in the right hindlimb after QPS. In contrast, it increased by 18 % on average in the left hindlimb after QPS. The average MEP was higher for the right hindlimb than the left hindlimb at all post-stimulus time points, with a significant difference in the MEP amplitudes between limbs over time ( $p = 9.23 \times 10^{-7}$ , two-way ANOVA). Fig. 6(b) shows that the normalized MEP amplitudes after sham conditioning (without QPS) were 90% and 93% of the baseline on average in the left and right hindlimbs, respectively, showing no

changes from the baseline. No significant difference was observed between limbs (p=0.554).

#### 4. Discussion

### 4.1. Coil implantation

We successfully demonstrated neuromodulation by magnetic stimulation using an implantable coil placed on the cortex without penetrating the cortical tissue. By placing the coil in contact with the cortical surface epidurally, the current intensity required for stimulation was considerably lower than that used in LI-rTMS by minimizing the attenuation of the electric field due to the distance between the coil and the stimulation target. It also enabled focal stimulation by minimizing electric field dispersion. Notably, our epidural approach showed the feasibility of magnetic stimulation in a focal region without penetrating the cortex. Specifically, a figure-eight coil, a representative coil shape that allowed focal TMS, generates an electric field in a region where the coil partially overlaps. However, even in a non-overlapped area exceeding 200 mm², the electric field is generated with a significant strength, considerable to the overlapped area [49]. While it is possible to

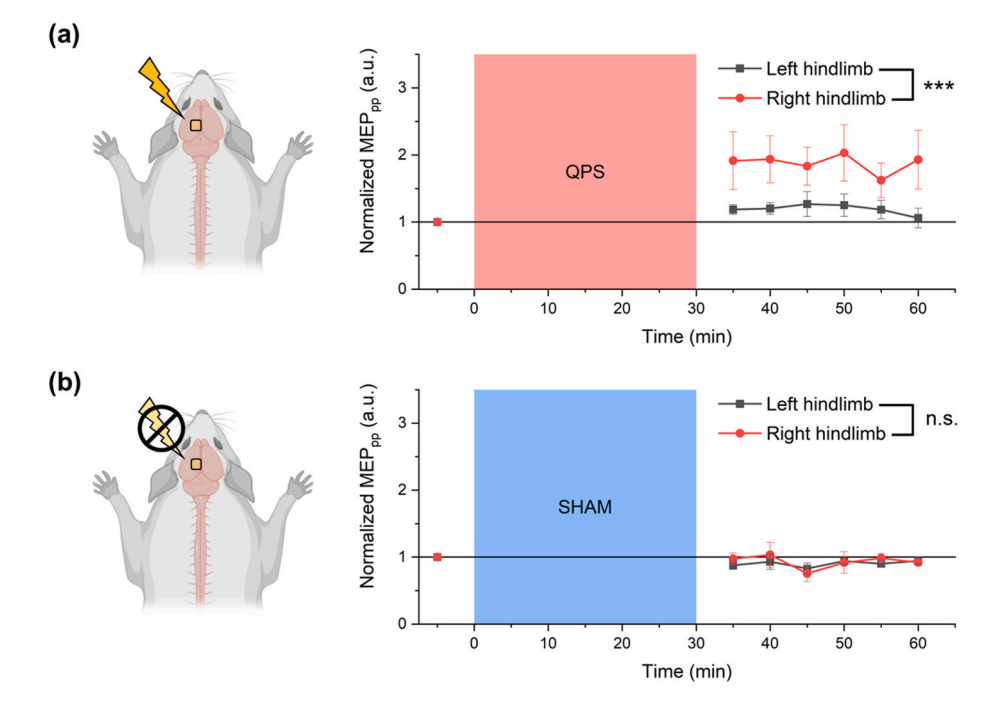


**Fig. 6.** Time courses of normalized MEPs. (a) When QPS (n = 5) was applied to the left motor cortex, the potentiation of MEP amplitudes was observed in the right hindlimb (p < 0.001, two-way ANOVA between the right and left limbs). (b) The control group (n = 4) showed no significant difference between hindlimbs (p > 0.05). The symbols represent the mean, and the whiskers represent the standard error of the mean.

achieve strong and focal enough stimulation within a specific small area, there remains a risk of cortical stimulation induced by subthreshold stimulation within the non-covered area by the coil [4]. Conversely, epidural stimulation induces electric fields only in the area directly beneath the coil, thus minimizing the risk of unintended stimulation. This area is approximately  $12\,\mathrm{mm}^2$  in size, roughly 1/16th the size of the area affected by TMS in previous studies. In addition, fixing the coil to the skull using dental resin helped resolve the issue of unstable coil positioning for long-term stimulation, one of the major issues commonly encountered in TMS. Our method of implanting a coil that uses a low-intensity current also has merit in that discomforts such as scalp sensation and pain caused by the high-intensity current in TMS could be significantly alleviated [50]. Moreover, it is expected to be able to stimulate even sulcal areas by placing the coil on the gyrencephalic cortex

By implanting the coil, we achieved the highly improved focality compared to previous studies as illustrated in Fig. 7. The electric field focality,  $S_{1/2}$ , was calculated based on the definition from a study of TMS coil designs [2]. Compared with the studies on LI-rTMS or TMS, our approach improved the focality by at least 8 up to 23 times. The distributions of normalized electric fields also showed clear distinction in focality as illustrated in Fig. 7.

### 4.2. MEP modulation

Magnetically stimulating the left motor cortex through the implanted coil caused the amplitude of MEPs in the right hindlimb to increase by 88 % after QPS compared to the baseline. This potentiation effect was clearly greater than that in the left hindlimb corresponding to the

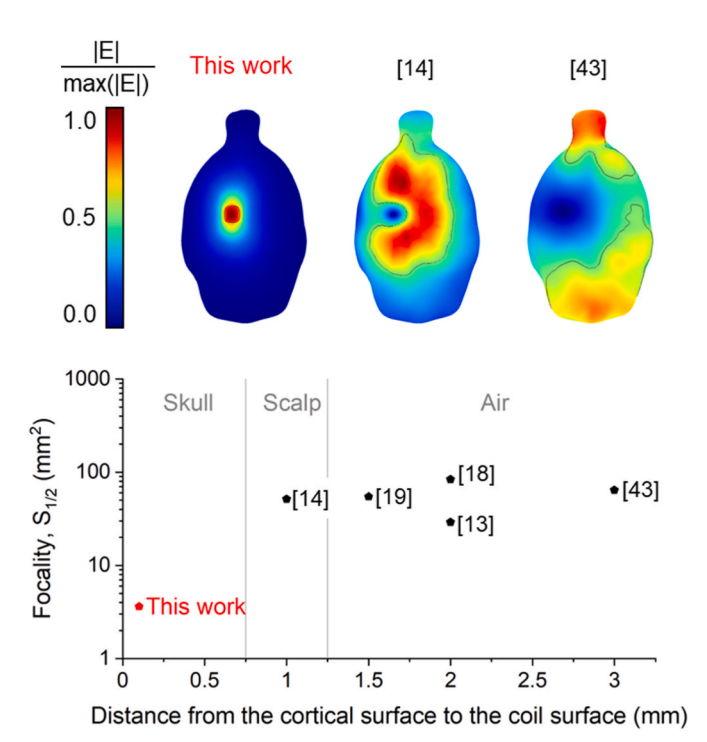


**Fig. 7.** Comparison of the focality of magnetic stimulation as a function of the distance from the cortical surface to the coil surface, based on this and previous studies [13,14,18,19,43]. The electric field focality  $S_{1/2}$  is defined based on a previous study [2], which quantifies the half-value spread. By adapting the coil dimensions and the distance between the coil and the cortex from each reference, the focality is calculated in the computational simulation setup. For epidural magnetic stimulation (this study), LI-rTMS [14] and TMS [43], the color maps represent the normalized electric field distributions on the cortical surface. (For interpretation of the references to color in this figure legend, the reader is referred to the Web version of this article.)

ipsilateral side of the stimulated region, consistent with previous studies on QPS [44,45]. In the control group, which had a coil implanted but was not given QPS, no change in MEP amplitude was observed in both hindlimbs. These results confirmed the feasibility of magnetic stimulation using an implantable coil to modulate MEPs.

In the QPS group, the MEP amplitude of the left hindlimb, the ipsilateral side of the stimulation site, was also slightly increased by 18 % on average compared to the baseline. Unintended stimulation by the coil might have caused this increase because the motor cortex region for the hindlimb is located right next to the midline of the cortex [38]. During surgical procedures, the cranial window was opened larger than the size of the coil to guarantee contact between the coil and cortex. Therefore, it is hypothesized that this margin would have caused the mispositioning of the coil at the stage of fixing it using dental resin. Another hypothesis is that during stimulation, the interhemispheric interactions via the corpus callosum inadvertently partially stimulated the contralateral motor cortex [51]. Tsutsumi et al. reported a similar phenomenon that QPS with an inter-stimuli interval of 5 ms, the same parameter used in our study, increased the MEP amplitudes from both the left and right dorsal interosseous after stimulation of the left motor cortex, with the increase higher in the contralateral side than in the ipsilateral side [52]. Nevertheless, it was evident that the targeted cortical region was stimulated by the increase in MEP amplitude being significantly higher for the contralateral hindlimb than for the ipsilateral hindlimb.

The current amplitude we used for magnetic stimulation was 6 A, which is two to three orders lower than those used in TMS and LI-rTMS. Such a significant reduction in current amplitude was achieved through the use of a high-inductance coil and epidural implantation. The electric field intensities induced by the coil could be increased by increasing the current or the inductance [53]. Since the coil used in our experiments had an inductance of 1 mH, which is twofold higher than commercial TMS coils, it was possible to stimulate with a much lower current [28]. Bringing the coil into contact with the cortical surface also contributed to lowering the current since it minimized the attenuation of the electric field induced by the coil over distance. Therefore, it was possible to obtain an electric field intensity similar to that used in LI-rTMS and demonstrate potentiation effects comparable to those reported in LI-rTMS studies [14,19].

# 4.3. Thermal safety

By measuring the heating of the coil surface, the stimulation intensity was determined so that the cortex was not thermally damaged even when stimulation was applied continuously for a certain period. Since the rising phase of a monophasic pulse is known to cause magnetic stimulation [54], the energy consumed by the coil could be minimized by shortening the falling phase. Fig. 2(a) shows that the time to fall from 95% to 5% of the peak is  $25~\mu s$  and  $550~\mu s$  for the implantable and TMS coils, respectively. The falling time of the pulse used for the implantable coil was significantly reduced to less than one-twentieth of that used for TMS. However, the strategy of minimizing the energy consumed in the coil by shortening the falling time does not apply to TMS due to the differences in the pulse-generating systems used in TMS and our study. In our study, the shape of pulses could be modified flexibly by configuring a function generator and a signal amplifier due to the lower current than TMS. However, a capacitive charging and discharging method is used to generate a high current pulse in the kA range in TMS, inevitably leading to a long falling time for discharging from the coil [55]. Several strategies have been suggested to resolve these limitations of TMS, such as pulse width modulation or phase control [5,31–33].

In addition to reducing the energy consumed in the coil by designing the optimal stimulation pulses, we also suggested a stimulation protocol to prevent heat accumulation, thereby avoiding thermal damage to the cortex. Previous LI-rTMS studies used stimulation protocols in which 1800 to 6000 pulses were applied over a short period at a rate of 600 pulses per minute [14,16,56]. However, these protocols were unsuitable

for use with the implanted coil since excessive heat could be accumulated. Instead, in our experiments, the QPS protocol applied 1440 pulses at 48 pulses per minute for 30 min. Consequently, while the total number of applied pulses was similar to that used in previous studies, it was possible to suppress heat accumulation for an extended period by lowering the pulse rate per minute. By optimizing the parameters of the stimulation protocol, we successfully demonstrated that controlling heat generation during epidural magnetic stimulation was possible.

### 4.4. Possibilities and limitations of epidural magnetic stimulation

We for the first time demonstrated that the epidural implantation of a coil for magnetic stimulation of the brain is possible with a current level not exceeding the thermal safety limit, by minimizing the coil as well as by carefully optimizing magnetic stimulation protocol. Full implantation of a coil for magnetic stimulation of the brain, without penetrating the cortical tissue or durectomy, was first demonstrated.

Our proposed method distinguishes itself from other brain modulation techniques in that implantable devices provide superior spatial resolution and sustained stimulation delivery, albeit with some invasiveness-related risks. While transcranial direct current stimulation (tDCS) offers noninvasive stimulation with low intensity, its spatial precision is limited due to the induced electric field covering the broad cortical regions. Intracortical stimulation provides better spatial resolution but involves irreversible cortical tissue damage upon device implantation. In contrast, epidural magnetic stimulation involves only a craniectomy for precise cortical placement of the coil, allowing for inducing high-intensity electric field without cortical tissue damage and enabling focused stimulation. This spatial superiority of epidural stimulation is illustrated in Fig. 8 compared to transcranial and intracortical stimulation.

Some concerns may raise because of the inclusion of craniectomy in the implantation process. We want to emphasize that safely fixing the coil to a target cortical area through implantation enables continuous stimulation of the desired cortical region over a prolonged period. This approach eliminates the need to locate the stimulation site anew for each session, a limitation present in non-invasive methods such as TMS or tDCS. By eliminating positioning errors, consistent stimulation can be delivered to the target region even over years without requiring manual restraint or anesthesia. This approach based on implantation is feasible because we introduced a subthreshold stimulation method that avoids heat-induced damage to the cortical tissue near the coil. Moreover, challenges such as degradation of stimulation performance in intracortical electrodes due to immune responses can be overcome. Additionally, unlike intracortical electrical stimulation methods, epidural

stimulation does not damage cortical tissue. These significant advantages enable long-term tracking of responses to magnetic stimulation within the cortex in animal models, such as freely moving rodents.

There might be a concern that electrical stimulation would be more power efficient than magnetic stimulation. Conventional epidural electrical stimulation typically utilizes multiple small electrodes or arrays of electrodes, providing high power efficiency due to the use of low currents in the milliamperes range [58–60]. However, impedance changes due to immune responses around the electrodes can impact the consistency of stimulation intensity. Additionally, the need for at least two electrodes often results in a broader stimulation area, affecting larger cortical regions than intended. In contrast, implanted magnetic coils require higher currents in the amperes range to generate a sufficiently high electric field for neuronal modulation. This can cause significant heating, but we successfully demonstrated that careful optimization of the coil and stimulation parameters can help manage this issue. Unlike electrical stimulation, magnetic stimulation avoids the direct contact of electrically conducting part of the device with the target tissue, reducing the risk of immune responses and tissue damage, offering a more controlled and localized approach.

To power an implanted coil with high amplitude currents, practical options include using a wired connection or a battery-based device. For rodent studies, a wired connection can be straightforward and reliable, allowing continuous stimulation without issues. Alternatively, a battery could offer more freedom of movement, though it needs to be managed very carefully in terms of energy efficiency. Wireless power transmission is another potential approach but may introduce challenges such as electromagnetic interference, which could affect the stimulation efficacy. Thus, additional research efforts are required to overcome these challenges and ensure the reliability and efficiency of power delivery systems for implanted coils.

A single coil may not be adequate for stimulation of multiple cortical areas or higher intensity stimulation. Implementing multiple coils can offer several advantages. For instance, it allows for selective stimulation of various cortical regions without physically moving the coils, as demonstrated in a previous study [61]. Additionally, by adjusting the orientation of the electric field induced by each coil, it is possible to enhance the overall stimulation intensity through the principle of superposition. This approach can create a more potent electric field by simultaneously stimulating adjacent coils. To effectively utilize multiple coils, further study is needed to address several key considerations such as optimal device placement and alignment, heat and power management, and methods for effectively controlling multiple coils.

The increased distance to the target cortical region due to thicker dura in larger animal models can lead to a reduction in stimulation

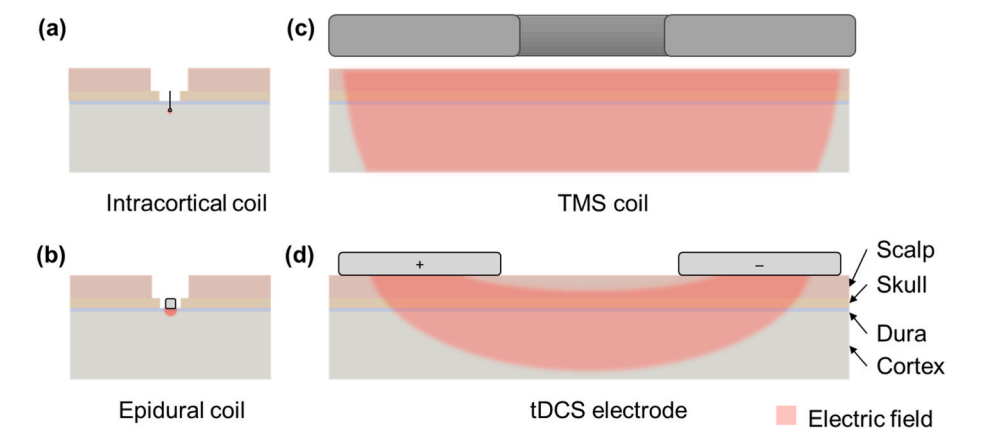


**Fig. 8.** Comparison of spatial extent of induced electric field by different magnetic stimulation methods. Placement of coils and electrodes, along with the extents of the induced electric field in cortical regions, are illustrated. The electric fields induced by magnetic stimulation using an (a) intracortical coil and (b) epidural coil are shown to be localized near at the coil surfaces. In contrast, the electric fields induced by (c) magnetic stimulation using a TMS coil and (d) electrical stimulation using tDCS surface electrodes cover a larger area. The size of coils and electrodes are scaled based on the previously reported values [8,43,57].

intensity and effectiveness. To address this challenge, a few strategies can be considered. One approach is to use an array of multiple coils arranged in a specific configuration to enhance the electric field strength at the target site. Another possibility is to improve the physical properties or design of the coil itself to allow stimulation to be delivered effectively while better penetrating the thicker dura. For instance, if the coil current is kept the same as used in our study, a larger coil can induce a stronger electric field and thus, can penetrate to a deeper site through a thicker dura, lowering the heat generation by the coil, which is even better in terms of thermal safety. These strategies however require further studies and optimization of the coil depending on animal models.

Epidural magnetic stimulation holds significant potential in clinical applications, particularly for patients at risk from invasive procedures, such as the insertion of electrodes into cortical tissue. One promising use could be in promoting motor function recovery in stroke patients. Epidural magnetic stimulation can deliver precise stimulation to the motor cortex without the need for direct cortical penetration, thereby reducing the risk of cortical damage. In addition to motor recovery, epidural magnetic stimulation can also be used to selectively target cortical areas responsible for abnormal neural activity in patients with neuropathic pain or focal epilepsy. By providing targeted stimulation without damaging cortical tissues, epidural magnetic stimulation has the potential to enhance neural plasticity and support neuronal recovery [15,16]. In research settings, epidural magnetic stimulation enables the modulation of specific brain regions, making it an excellent tool for studying cortical plasticity. Its focused, localized stimulation, in contrast to broader stimulation by TMS, can provide deeper insights into brain functions, supporting both clinical and experimental applications in neuroscience. These attributes underscore its potential for targeted and chronic neuromodulation while addressing concerns related to safety and efficacy.

### 5. Conclusion

This study introduces a novel method for neuromodulation using an epidurally implanted coil for focal magnetic stimulation of the brain. By positioning the coil directly on the cortical surface, we achieved focal stimulation with reduced current intensities in the range of amperes, ensuring that the temperature rise due to the stimulus current remained within the thermal safety limit. Our approach enhances the spatial resolution compared to non-invasive methods such as TMS and avoids the need for cortical penetration, reducing the risk of cortical tissue damage. The stable fixation of the coil allows for long-term, consistent stimulation of a focused target area without the need for repeated realignment and calibration. These findings suggest that the proposed epidural magnetic stimulation is promising not only for studying neuroplasticity but also for potential clinical applications.

# CRediT authorship contribution statement

**Kyeong Jae Lee:** Writing – original draft, Visualization, Validation, Methodology, Investigation, Formal analysis, Data curation, Conceptualization. **Jae-Won Jang:** Methodology, Investigation. **June Sic Kim:** Writing – review & editing, Validation, Funding acquisition. **Sohee Kim:** Writing – review & editing, Validation, Supervision, Resources, Project administration, Funding acquisition, Conceptualization.

### Declaration of competing interest

The authors declare that they have no known competing financial interests or personal relationships that could have appeared to influence the work reported in this paper.

# Acknowledgement

This research was supported by the Challengeable Future Defense

Technology Research and Development Program through the Agency for Defense Development (ADD) of Korea (No. 915069201). The authors would like to thank Professor Han Kyoung Choe for the advice regarding physiological analysis, D.V.M. Dong-Jae Kim for advices and technical support with veterinary knowledge regarding animal experiments, and Professor Shelley Fried at Massachusetts General Hospotal for the helpful discussions. The authors also would like to thank the Center for Core Research Facilities (CCRF) and Laboratory Animal Resource Center (LARC) at DGIST. Figs. 1, 2, and 6 were created with BioRender.

### References

- Drakaki M, Mathiesen C, Siebner HR, Madsen K, Thielscher A. Database of 25 validated coil models for electric field simulations for TMS. Brain Stimul 2022;15 (3):697–706.
- [2] Deng ZD, Lisanby SH, Peterchev AV. Electric field depth-focality tradeoff in transcranial magnetic stimulation: simulation comparison of 50 coil designs. Brain Stimul 2013;6(1):1–13.
- [3] Uwe H, Carlos S-L, Arthur PW, Cyrill Axel T, Henrik W, et al. The navigation of transcranial magnetic stimulation. Psychiatry Res Neuroimaging 2001;108(2): 123–31.
- [4] Funke K. Transcranial magnetic stimulation of rodents. In: Handbook of in vivo neural plasticity techniques; 2018. p. 365–87.
- [5] Peterchev AV, Goetz SM, Westin GG, Luber B, Lisanby SH. Pulse width dependence of motor threshold and input-output curve characterized with controllable pulse parameter transcranial magnetic stimulation. Clin Neurophysiol 2013;124(7): 1364-72
- [6] Barker AT, Garnham CW, Freeston IL. Magnetic nerve stimulation: the effect of waveform on efficiency, determination of neural membrane time constants and the measurement of stimulator output. Electroencephalogr Clin Neurophysiol Suppl 1991;43:227–37.
- [7] Bonmassar G, Lee SW, Freeman DK, Polasek M, Fried SI, Gale JT. Microscopic magnetic stimulation of neural tissue. Nat Commun 2012;3(1):921.
- [8] Lee SW, Fallegger F, Casse BDF, Fried SI. Implantable microcoils for intracortical magnetic stimulation. Sci Adv 2016;2(12):e1600889.
- [9] Kosta P, Mize J, Warren DJ, Lazzi G. Simulation-based optimization of figure-ofeight coil designs and orientations for magnetic stimulation of peripheral nerve. IEEE Trans Neural Syst Rehabil Eng 2020;28(12):2901–13.
- [10] Saha R, Sanger Z, Bloom RP, Benally OJ, Wu K, Tonini D, et al. Micromagnetic stimulation (μMS) dose-response of the rat sciatic nerve. J Neural Eng 2023;20(3): 036022
- [11] Moretti J, Rodger J. A little goes a long way: neurobiological effects of low intensity rTMS and implications for mechanisms of rTMS. Curr Res Neurobiol 2022;3:100033.
- [12] Rodger J, Mo C, Wilks T, Dunlop SA, Sherrard RM. Transcranial pulsed magnetic field stimulation facilitates reorganization of abnormal neural circuits and corrects behavioral deficits without disrupting normal connectivity. Faseb J 2012;26(4): 1593–606.
- [13] Makowiecki K, Harvey AR, Sherrard RM, Rodger J. Low-intensity repetitive transcranial magnetic stimulation improves abnormal visual cortical circuit topography and upregulates BDNF in mice. J Neurosci 2014;34(32):10780–92.
- [14] Tang AD, Lowe AS, Garrett AR, Woodward R, Bennett W, Canty AJ, et al. Construction and evaluation of rodent-specific rTMS coils. Front Neural Circ 2016; 10:47.
- [15] Tang AD, Bennett W, Bindoff AD, Bolland S, Collins J, Langley RC, et al. Subthreshold repetitive transcranial magnetic stimulation drives structural synaptic plasticity in the young and aged motor cortex. Brain Stimul 2021;14(6): 1498–507.
- [16] Boyer M, Baudin P, Stengel C, Valero-Cabre A, Lohof AM, Charpier S, et al. In vivo low-intensity magnetic pulses durably alter neocortical neuron excitability and spontaneous activity. J Physiol 2022;600(17):4019–37.
- [17] Khalifa A, Abrishami SM, Zaeimbashi M, Tang AD, Coughlin B, Rodger J, et al. Magnetic temporal interference for noninvasive and focal brain stimulation. J Neural Eng 2023;20(1).
- [18] Khokhar FA, Voss LJ, Steyn-Ross DA, Wilson MT. Design and demonstration in vitro of a mouse-specific transcranial magnetic stimulation coil. IEEE Trans Magn 2021; 57(7):1–11.
- [19] Jiang W, Isenhart R, Liu CY, Song D. A C-shaped miniaturized coil for transcranial magnetic stimulation in rodents. J Neural Eng 2023;20(2).
- [20] Khalifa A, Zaeimbashi M, Zhou TX, Abrishami SM, Sun N, Park S, et al. The development of microfabricated solenoids with magnetic cores for micromagnetic neural stimulation. Microsyst Nanoeng 2021;7:91.
- [21] Liu X, Whalen AJ, Ryu SB, Lee SW, Fried SI, Kim K, et al. MEMS micro-coils for magnetic neurostimulation. Biosens Bioelectron 2023;227:115143.
- [22] Ryu SB, Paulk AC, Yang JC, Ganji M, Dayeh SA, Cash SS, et al. Spatially confined responses of mouse visual cortex to intracortical magnetic stimulation from microcoils. J Neural Eng 2020;17(5):056036.
- [23] Lee JI, Seist R, McInturff S, Lee DJ, Brown MC, Stankovic KM, et al. Magnetic stimulation allows focal activation of the mouse cochlea. Elife 2022;11.
- [24] Bernardo R, Rodrigues A, Dos Santos MPS, Carneiro P, Lopes A, et al. Novel magnetic stimulation methodology for low-current implantable medical devices. Med Eng Phys 2019;73:77–84.

- [25] Park HJ, Seol JH, Ku J, Kim S. Computational study on the thermal effects of implantable magnetic stimulation based on planar coils. IEEE Trans Biomed Eng 2016;63(1):158–67.
- [26] Matsumi N, Kengo M, Nobuya M, Eiji M, Tomohisa F, Akira N, et al. Thermal damage threshold of brain tissue —histological study of heated normal monkey brains. Neurol Med -Chir 1994;34(4). 209-15.
- [27] ISO 14708-1. Implants for surgery active implantable medical devices Part 1: general requirements for safety, marking and for information to be provided by the manufacturer International Standard. 2014.
- [28] Lee KJ, Park B, Jang J-W, Kim S. Magnetic stimulation of the sciatic nerve using an implantable high-inductance coil with low-intensity current. J Neural Eng 2023;20 (3):036035
- [29] MagPro R20 User Guide, MagVenture.
- [30] Sommer M, Alfaro A, Rummel M, Speck S, Lang N, Tings T, et al. Half sine, monophasic and biphasic transcranial magnetic stimulation of the human motor cortex. Clin Neurophysiol 2006;117(4):838–44.
- [31] Peterchev AV, Jalinous R, Lisanby SH. A transcranial magnetic stimulator inducing near-rectangular pulses with controllable pulse width (cTMS). IEEE Trans Biomed Eng. 2008;55(1):257–66.
- [32] Kagan ZB, Mize JT, Kosta P, Lazzi G, Normann RA, Warren DJ. Reduced heat generation during magnetic stimulation of rat sciatic nerve using current waveform truncation. IEEE Trans Neural Syst Rehabil Eng 2019;27(5):937–46.
- [33] Wang B, Zhang J, Li Z, Grill WM, Peterchev AV, Goetz SM. Optimized monophasic pulses with equivalent electric field for rapid-rate transcranial magnetic stimulation. J Neural Eng 2023;20(3).
- [34] Minusa S, Osanai H, Tateno T. Micromagnetic stimulation of the mouse auditory cortex in vivo using an implantable solenoid system. IEEE Trans Biomed Eng 2017; 65(6):1301–10.
- [35] Tim W, Felipe F, Uri E, Ciro R-E, Alan G, Markus Z, et al. Transcranial magnetic stimulation and stroke: a computer-based human model study. Neuroimage 2006; 30(3):857–70
- [36] Paxinos G, Watson C. The rat brain in stereotaxic coordinates. sixth ed. Academic Press: 2008.
- [37] Robert DH, Ernest PL. Organization of motor and somatosensory neocortex in the albino rat. Brain Res 1974;66(1):23–38.
- [38] Ebbesen CL, Insanally MN, Kopec CD, Murakami M, Saiki A, Erlich JC. More than just a "motor": recent surprises from the frontal cortex. J Neurosci 2018;38(44): 0402-132
- [39] Yang P, Wang Z, Zhang Z, Liu D, Manolios EN, Chen C, et al. The extended application of the Rat Brain in Stereotaxic Coordinates in rats of various body weight. J Neurosci Methods 2018;307:60–9.
- [40] Beom J, Lee JC, Paeng JC, Han TR, Bang MS, Oh BM. Repetitive transcranial magnetic stimulation to the unilateral hemisphere of rat brain. J Vis Exp 2016:116.
- [41] Gersner R, Paredes C, Hameed MQ, Dhamne SC, Pascual-Leone A, Rotenberg A. Transcranial magnetic stimulation tracks subminute changes in cortical excitability during propofol anesthesia. Ann Clin Transl Neurol 2020;7(3):384–9.
- [42] Luft AR, Kaelin-Lang A, Hauser TK, Cohen LG, Thakor NV, Hanley DF. Transcranial magnetic stimulation in the rat. Exp Brain Res 2001;140(1):112–21.
- [43] Parthoens J, Verhaeghe J, Servaes S, Miranda A, Stroobants S, Staelens S. Performance characterization of an actively cooled repetitive transcranial magnetic stimulation coil for the rat. Neuromodulation 2016;19(5):459–68.

- [44] Hamada M, Ugawa Y. Quadripulse stimulation—a new patterned rTMS. Restor Neurol Neurosci 2010;28(4):419–24.
- [45] Matsumoto H, Ugawa Y. Quadripulse stimulation (QPS). Exp Brain Res 2020;238 (7–8):1619–25.
- [46] Park HJ, Kang H, Jo J, Chung E, Kim S. Planar coil-based contact-mode magnetic stimulation: synaptic responses in hippocampal slices and thermal considerations. Sci Rep 2018;8(1):13423.
- [47] Rotenberg A, Muller PA, Vahabzadeh-Hagh AM, Navarro X, Lopez-Vales R, Pascual-Leone A, et al. Lateralization of forelimb motor evoked potentials by transcranial magnetic stimulation in rats. Clin Neurophysiol 2010;121(1):104–8.
- [48] Kamida T, Fujiki M, Hori S, Isono M. Conduction pathways of motor evoked potentials following transcranial magnetic stimulation: a rodent study using a "Figure- 8" coil. Muscle Nerve 1998;21(6):722–31.
- [49] Wagner T, Rushmore J, Eden U, Valero-Cabre A. Biophysical foundations underlying TMS: setting the stage for an effective use of neurostimulation in the cognitive neurosciences. Cortex 2009;45(9):1025–34.
- [50] Peterchev AV, Luber B, Westin GG, Lisanby SH. Pulse width affects scalp sensation of transcranial magnetic stimulation. Brain Stimul 2017;10(1):99–105.
- [51] Benali A, Trippe J, Weiler E, Mix A, Petrasch-Parwez E, Girzalsky W, et al. Thetaburst transcranial magnetic stimulation alters cortical inhibition. J Neurosci 2011; 31(4):1193-203
- [52] Tsutsumi R, Hanajima R, Terao Y, Shirota Y, Ohminami S, Shimizu T, et al. Effects of the motor cortical quadripulse transcranial magnetic stimulation (QPS) on the contralateral motor cortex and interhemispheric interactions. J Neurophysiol 2014;111(1):26–35.
- [53] Reuter C, Battocletti JH, Myklebust J, Maiman D. Magnetic stimulation of peripheral nerves. In: Conf proc IEEE eng med biol soc. New Orleans, LA, USA; 1988. p. 928–9.
- [54] Corthout E, Barker AT, Cowey A. Transcranial magnetic stimulation. Which part of the current waveform causes the stimulation? Exp Brain Res 2001;141(1):128–32.
- [55] Miniussi C, Paulus W, Rossini PM. Transcranial brain stimulation. CRC Press; 2012.
- [56] Heath A, Lindberg DR, Makowiecki K, Gray A, Asp AJ, Rodger J, et al. Mediumand high-intensity rTMS reduces psychomotor agitation with distinct neurobiologic mechanisms. Transl Psychiatry 2018;8(1):126.
- [57] Thair H, Holloway AL, Newport R, Smith AD. Transcranial direct current stimulation (tDCS): a beginner's guide for design and implementation. Front Neurosci 2017;11:641.
- [58] Adkins DL, Campos P, Quach D, Borromeo M, Schallert K, Jones TA. Epidural cortical stimulation enhances motor function after sensorimotor cortical infarcts in rats. Exp Neurol 2006;200(2):356–70.
- [59] Levy R, Ruland S, Weinand M, Lowry D, Dafer R, Bakay R. Cortical stimulation for the rehabilitation of patients with hemiparetic stroke: a multicenter feasibility study of safety and efficacy. J Neurosurg 2008;108(4):707–14.
- [60] Cherney LR, Harvey RL, Babbitt EM, Hurwitz R, Kaye RC, Lee JB, Small SL. Epidural cortical stimulation and aphasia therapy. Aphasiology 2012;26(9): 1192–217.
- [61] Minusa S, Muramatsu S, Osanai H, Tateno T. A multichannel magnetic stimulation system using submillimeter-sized coils: system development and experimental application to rodent brain in vivo. J Neural Eng 2019;16(6):066014.